Experimental Dermatology ADF

Inhibition of fatty acid amide hydrolase exerts cutaneous anti-inflammatory effects both in vitro and in vivo

Journal:	*Experimental Dermatology*
Manuscript ID	EXD-15-0327.R1
Manuscript Type:	Letter to the Editors
Date Submitted by the Author:	17-Nov-2015
Complete List of Authors:	Oláh, Attila; University of Debrecen, Department of Physiology Ambrus, Lídia; University of Debrecen, Department of Physiology Nicolussi, Simon; University of Bern, Institute of Biochemistry and Molecular Medicine, NCCR TransCure Gertsch, Jürg; University of Bern, Institute of Biochemistry and Molecular Medicine, NCCR TransCure Tubak, Vilmos; Creative Laboratory Ltd, Kemény, Lajos; University of Szeged, Department of Dermatology and Allergology; University of Szeged, Dermatological Research Group of the Hungarian Academy of Sciences Soeberdt, Michael; Dr. August Wolff GmbH & Co. KG Arzneimittel, Medical Affairs Abels, Christoph; Dr. August Wolff GmbH&Co. KG Arzneimittel.de, Medical Affairs Biro, Tamas; University of Debrecen, Physiology; University of Debrecen, Department of Immunology
Keywords:	fatty acid amide hydrolase, endocannabinoid system, human keratinocytes, inflammation, Toll-like receptors

Inhibition of fatty acid amide hydrolase exerts cutaneous anti-inflammatory effects both *in vitro* and *in vivo*

Attila Oláh[1], Lídia Ambrus[1], Simon Nicolussi[2], Jürg Gertsch[2], Vilmos Tubak[3], Lajos Kemény[4], Michael Soeberdt[5], Christoph Abels[5], Tamás Bíró[1,6]

[1]DE-MTA "Lendület" Cellular Physiology Research Group, Department of Physiology, Faculty of Medicine, University of Debrecen, Debrecen, Hungary; [2]Institute of Biochemistry and Molecular Medicine, NCCR TransCure, University of Bern, Bern, Switzerland; [3]Creative Laboratory Ltd., Szeged, Hungary; [4]MTA-SZTE Dermatological Research Group, University of Szeged, Szeged, Hungary; [5]Dr. August Wolff GmbH & Co. KG Arzneimittel, Bielefeld, Germany; [6]Department of Immunology, Faculty of Medicine, University of Debrecen, Debrecen, Hungary

Corresponding author

Tamás Bíró, M.D., Ph.D., D.Sc.

4032 Debrecen, Nagyerdei krt. 98., Hungary

E-mail: biro.tamas@med.unideb.hu

Phone: +36-52-255-575

FAX: +36-52-255-116.

To the Editor

Background

Numerous studies introduced epidermal keratinocytes as "non-classical" immune-competent cells, hence potent primary regulators and active participants of cutaneous immune functions (1, s1-6). Therefore, targeting them might provide a novel, highly specific anti-inflammatory therapeutic possibility. The endocannabinoid system (ECS) is an emerging signaling network which regulates multiple cutaneous functions (2,3). The loss of homeostatic endocannabinoid (eCB) signaling of epidermal keratinocytes was shown to dramatically enhance inflammatory processes, arguing for that the cutaneous eCB tone plays a "gate-keeper" role in the initiation phase of skin inflammation (4; for further details see **Supplementary Background section**). Moreover, elevation of the eCB tone, e.g. by the inhibition of fatty acid amide hydrolase (FAAH), the most important enzyme engaged with the degradation of the eCB anandamide (AEA; 5), exerts ECS-mediated anti-inflammatory actions in multiple organs (5).

Questions addressed

Based on these data we hypothesized that up-regulation of expression/activity of FAAH (thereby decreasing the eCB tone, and increasing the level of the pro-inflammatory "eCB degradation product" arachidonic acid [AA]) might contribute to the development of the inflammatory processes. Therefore, we aimed at investigating (i) mRNA and protein expressions and activity of FAAH in human keratinocytes in Toll-like receptor (TLR)-induced inflammation models; and (ii) the suggested anti-inflammatory effects of two newly developed, potent and selective N-alkylcarbamate FAAH-inhibitors WOBE440 (IC_{50}=25±8 nM) and WOBE479 (IC_{50}=78±13 nM) (**Supplementary Figure S1**) which

show high specificity over other known targets within the ECS (IC_{50}>10 μM for cannabinoid receptor [CNR]-1, CNR2, monoacylglycerol lipase and the putative endocannabinoid membrane transporter) (6) on primary (NHEK) and immortalized (HPV-KER; 7,8) human epidermal keratinocytes as well as in NC/Tnd mice, a widely used animal model of atopic dermatitis (AD; 9).

Experimental design

Detailed description of the methods can be found in the **Supplementary Experimental design section**.

Cell culture

Human skin samples were obtained after obtaining written informed consent from healthy individuals, adhering to Helsinki guidelines, and after obtaining permissions from respective institutional and government bodies (protocol No.: DE OEC RKEB/IKEB 3724-2012; document No.: IX-R-052/01396-2/2012).

Determination of cellular viability, apoptosis and necrosis

Viability and cell death were determined by MTT and $DiIC_1(5)$-SYTOX Green assays as described previously (s11).

Expression analysis

Molecular expression was monitored by Q-PCR and Western blot as described previously with slight modifications (s11). The released amount of IL6 and IL8 was

determined using OptEIA kits (BD Pharmingen, Franklin Lakes, NJ, USA) according to the manufacturer's protocol.

Determination of the FAAH-activity

The enzymatic activity of FAAH in NHEKs and HPV-KERs homogenates was assessed by determination of the hydrolysis of [ethanolamine-1-^{3}H]AEA as previously described (s12-16).

Experiments on NC/Tnd mice

The study was conducted at BioTox Sciences (BTS; San Diego, CA, USA). The study design and animal usage were reviewed and approved by the Institutional Animal Care and Use Committee (IACUC; No. 1109-05). Clinical score was determined from observations of the upper back/lower neck with a scale of 0–3 (0: absent; 1: mild; 2: moderate; 3: severe) for erythema, edema or papulations, and for oozing, crusts or hemorrhages. Each mouse received a single daily topical dose that was applied to the upper back/lower neck area.

Statistical analysis

Data were analyzed and graphs were plotted by using Origin Pro Plus 6.0 software (Microcal, Northampton, MA, USA), using Student's two-tailed two samples *t*-test and $P<0.05$ values were regarded as significant differences.

Results

We found that FAAH is expressed in HPV-KERs both at the mRNA and protein levels (**Supplementary Figure S2**; **Figure 1a-b**). Importantly, we also found that upon administration of TLR2 or -4-activators (lipoteichoic acid [LTA] and lipopolysaccharide [LPS], respectively), expression of FAAH at the protein level tended to be increased. Interestingly, at the mRNA level, only 3-hr LPS treatment induced significant increase (**Figure 1a-b**; **Supplementary Figure S2**), and in NHEKs, only LTA was able to enhance the expression (**Figure 1c-d**). Importantly, both HPV-KERs and NHEKs exhibited significant elevations in FAAH-activity upon TLR2-activation (**Figure 1e-f**). The above findings raised the possibility that the decreased eCB mediated by FAAH up-regulation might theoretically contribute to the development of the TLR-activation-induced pro-inflammatory responses in the human skin. To challenge this hypothesis, next, we investigated the putative anti-inflammatory effects of selective FAAH-inhibitors, by monitoring the production of key pro-inflammatory cytokines (*IL1A*, *IL1B*, *IL6* and *IL8*; s17-19). As expected, both the commercially available FAAH-inhibitor URB597 (s20), as well as novel inhibitors (WOBE440 and WOBE479) almost completely prevented the LTA-induced up-regulation of the aforementioned cytokines (**Figure 2a-b**). Importantly, they also significantly suppressed the LTA-induced release of IL6 and IL8 (**Figure 2c-d**). FAAH-inhibitors exert their effects via the elevation of the local AEA tone, which subsequently activates CNR1 and CNR2 (5). In a good agreement with the literature data (4), combined antagonism of these receptors markedly abolished the anti-inflammatory actions of the FAAH-inhibitors (**Supplementary Figure S3**). Importantly, concentrations of FAAH-inhibitors having been proven to exert anti-inflammatory actions (i.e. 100 and 200 nM for WOBE440 and WOBE479, respectively) did not induce any

measurable cytotoxicity when applied either in short-term (8- and 24-hr; **Supplementary Figure S4a-d**), or in long-term experiments (72-hr; **Supplementary Figure S5a-b**), indicating that they can most probably be administered without the risk of significant cutaneous cytotoxicity. Finally, we aimed at investigating the putative *in vivo* efficiency of the FAAH-inhibitors, employing a widely accepted animal model of AD, i.e. the NC/Tnd mice (9). After appropriate antigen exposure and the development of AD-like cutaneous symptoms, mice were treated with the novel FAAH-inhibitors or vehicle, as described in the Supplementary Experimental Design section. As a "positive" control, tacrolimus ointment (Protopic®; commonly administered in the treatment of AD; s21) was used. Of great importance, FAAH-inhibitors significantly reduced both the total disease score (for details, see **Supplementary Experimental design** section) and ear thickness. It is also important to note that beneficial effects of the FAAH-inhibitors were comparable to those exerted by tacrolimus (**Figure 2e-f; Supplementary Figure S6a-d**), and that no (obvious macroscopic or behavioral) side-effects developed during the one month-long drug administration. These data strongly suggest that inhibition of FAAH results in substantial anti-inflammatory actions *in vivo* as well.

Conclusions

For detailed discussion, see **Supplementary Conclusion section 1.** Taken together, our results introduce FAAH as an important, TLR2-dependent regulator of cutaneous inflammatory processes (**Supplementary Figure S7a-b**). Thus, according to our translationally relevant, complementary *in vitro* and *in vivo* data, local inhibition of FAAH

could provide a highly targeted and hence most probably side-effect-free tool for mitigating cutaneous inflammation (further discussion of the expected beneficial effects can be found in the **Supplementary Conclusion section 2**). Therefore, these data should encourage one to test, next in appropriate clinical trials the *in vivo* efficiency of the FAAH-inhibitors in the management of inflammatory skin diseases, such as e.g. AD.

Acknowledgement

The research was supported by Hungarian ("Lendület" LP2011-003/2015, OTKA 101761, OTKA 105369, TÁMOP-4.2.4.A/2-11-1-2012-0001, TÁMOP-4.2.2./A-11/1/KONV-2012-0025) and German (ZIM KF2611301 MD0) research grants and by Dr. August Wolff GmbH & Co. KG Arzneimittel (Bielefeld, Germany). SN and JG were supported by NCCR TransCure, Switzerland. The authors are grateful to Judit Szabó-Papp, Dóra Bodnár, Erika Herczeg-Lisztes, Róbert L. Katona and Attila G. Szöllősi for their expert contributions.

Authors' contribution:

AO and LA performed *in vitro* experiments and analyzed the data. SN and JG performed FAAH activity assays. AO wrote the manuscript. AO, MS, CA and TB designed the research study, and all authors reviewed the manuscript. LK and VT provided HPV-KERs; MS and CA provided WOBE440 and WOBE479. All authors read and approved the final version of the manuscript.

Conflict of interest

This study was supported by an industrial research grant (see Acknowledgement), and two of the authors (MS and CA) are employees of the sponsor. AO was employed by the sponsor between 02/01/2014 and 01/31/2015.

REFERENCES

1. Metz M, Maurer M. Innate immunity and allergy in the skin. Curr Opin Immunol 2009: **21**: 687–693.
2. Bíró T, Tóth B I, Haskó G *et al.* The endocannabinoid system of the skin in health and disease: novel perspectives and therapeutic opportunities. Trends Pharmacol Sci 2009: **30**: 411–420.
3. Maccarrone M, Bab I, Bíró T *et al.* Endocannabinoid signaling at the periphery: 50 years after THC. Trends Pharmacol Sci 2015: **36**: 277–296.
4. Karsak M, Gaffal E, Date R *et al.* Attenuation of allergic contact dermatitis through the endocannabinoid system. Science 2007: **316**: 1494–1497.
5. Marzo V Di. Targeting the endocannabinoid system: to enhance or reduce? Nat Rev Drug Discov 2008: **7**: 438–455.
6. Nicolussi S, Chicca A, Rau M *et al.* Correlating FAAH and anandamide cellular uptake inhibition using N-alkylcarbamate inhibitors: From ultrapotent to hyperpotent. Biochem Pharmacol 2014: **92**: 669–689.
7. Polyanka H, Szabo K, Tax G *et al.* Characterization of UV-B induced cellular processes in a keratinocyte cell line (HPV-KER) immortalized with the HPV-E6 oncogene. J Invest Dermatol 2013: **133:(1)** S218.
8. Szegedi K, Göblös A, Bacsa S *et al.* Expression and Functional Studies on the Noncoding RNA, PRINS. Int J Mol Sci 2012: **14**: 205–225.

9. Jung K, Tanaka A, Fujita H *et al.* Peroxisome proliferator-activated receptor γ-mediated suppression of dendritic cell function prevents the onset of atopic dermatitis in NC/Tnd mice. J Allergy Clin Immunol 2011: **127**: 420–429.e1–6.

FIGURE LEGENDS

Figure 1 *Protein expression and activity of FAAH is up-regulated upon Toll-like receptor activation in immortalized (HPV-KER) and primary (NHEK) human epidermal keratinocytes*

(**a**-**d**) Western blot analysis of lysates of HPV-KERs (**a**) or NHEKs (**c**) treated with LPS, LTA (5 and 10 µg/ml, respectively) or vehicle (24 hrs). Two additional experiments yielded similar results. (**b**, **d**) Statistical analyses of the above Western blot experiments (**c**: HPV-KER; **d**: NHEK). OD: optical density of the FAAH bands normalized to the corresponding β-tubulin (TUBB) signals. Data are presented as mean±SEM of 3 independent experiments regarding vehicle control as 1 (solid line). **P*<0.05 vs. control group. (**e**-**f**) Measurement of FAAH-activity on HPV-KERs (**c**) and on NHEKs (**d**) following 24-hr treatments with LTA (10 µg/ml) or vehicle. Specific inhibition of FAAH activity ([^{3}H]AEA hydrolysis) was achieved with URB597 (100 nM). Data are expressed as mean±SEM of three independent experiments each of them performed in triplicates. **, *** *P*<0.01 and 0.001, respectively; n.s.: non-significant difference.

Figure 2 *FAAH-inhibitors exert significant anti-inflammatory actions both in vitro and in vivo*

(**a**-**b**) Q-PCR analyses of HPV-KERs following the indicated 24-hr treatments (LTA: 10 µg/ml; URB597: 100 nM; WOBE440: 100 nM; WOBE479: 200 nM). Data are presented by using ΔΔCT method regarding *PPIA*-normalized mRNA expressions of the vehicle control as 1 (solid line). Data are expressed as mean±SD of 3 independent determinations. Two additional experiments yielded similar results. (**c**-**d**) Determination of the released cytokine concentration following 24-hr treatments (LTA: 10 µg/ml;

WOBE440: 100 nM; WOBE479: 200 nM). Data are presented as mean±SEM of three independent determinations. One additional experiment yielded similar results. (**a**-**d**) **P*<0.05 compared to the vehicle control. #*P*<0.05 compared the LTA-treated, FAAH-inhibitor-free group. (**e**-**f**) Alterations in total ear thickness (**e**) and in total disease score (**f**) following the indicated treatments (tacrolimus: 0.1 [w/v]%; WOBE440 and -479: 1 [w/v]%). *, ** and *** mark significant (*P*<0.05, 0.01 or 0.001, respectively) differences of the graphs with the same color compared to the daily control group. N=8-9 animals were investigated in each group.

Supporting Information

Additional data (**Supplementary Background, Supplementary Experimental Design, Supplementary Conclusion sections 1-2, Supplementary Figures S1-7, Supplementary References s1-s29**) can be found in the Supporting Information.

Figure 1 – Protein expression and activity of FAAH is up-regulated upon Toll-like receptor activation in human keratinocytes

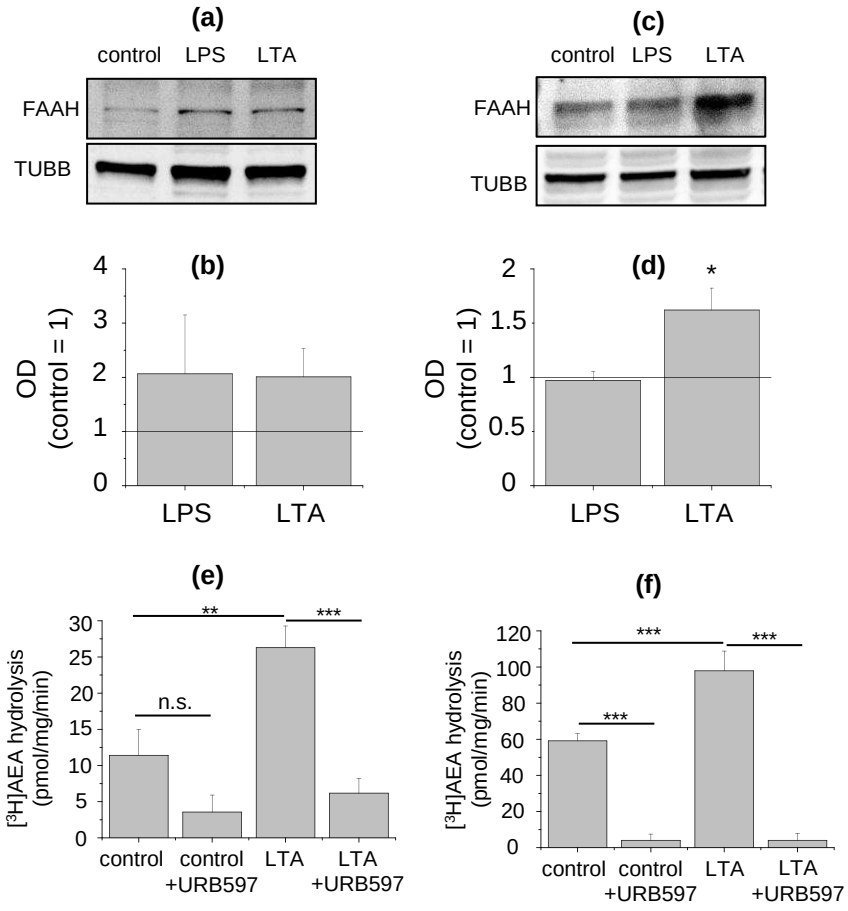

Figure 2 – FAAH-inhibitors exert remarkable anti-inflammatory actions both *in vitro* and *in vivo*

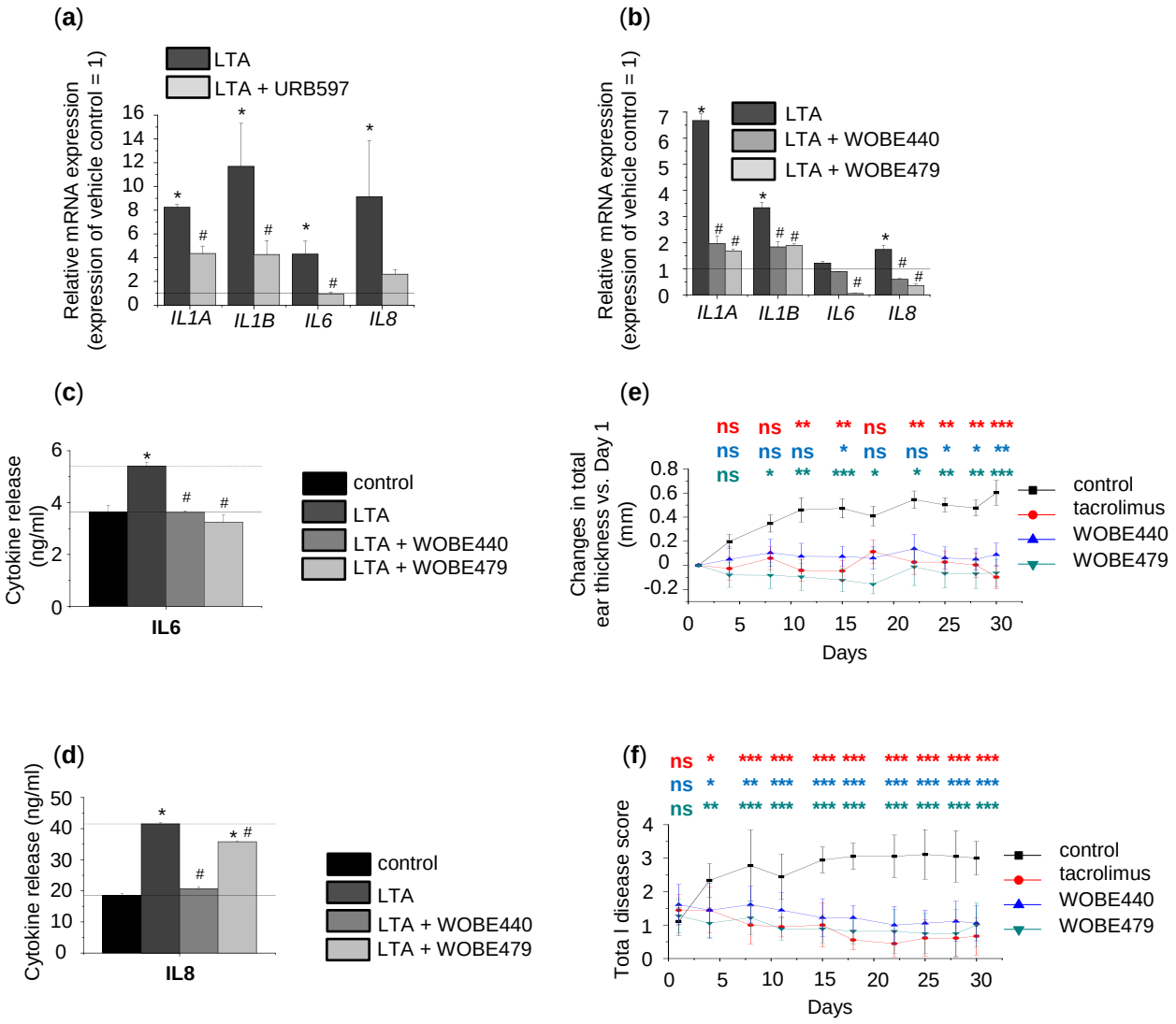

Inhibition of fatty acid amide hydrolase exerts cutaneous anti-inflammatory effects both *in vitro* and *in vivo*

Attila Oláh, Lídia Ambrus, Simon Nicolussi, Jürg Gertsch, Vilmos Tubak, Lajos Kemény, Michael Soeberdt, Christoph Abels, Tamás Bíró

SUPPLEMENTARY MATERIAL

Supplementary Background

The endocannabinoid system (ECS) is an emerging signaling network, which regulates multiple cutaneous functions (see reviewed in 2). Notably, by using mice lacking both CNR1 and CNR2 cannabinoid receptors, Karsak *et al.* have elegantly demonstrated that the loss of homeostatic endocannabinoid (eCB) signaling of epidermal keratinocytes dramatically enhanced cutaneous inflammatory processes (4). In line with these findings, the CNR1 receptor antagonist/inverse agonist falcarinol triggered the expression of the pro-inflammatory interleukin (IL)-8 and chemokine (C-C motif) ligand 2 (CCL2; also known as monocyte chemotactic protein 1, [MCP1]) in cultured human HaCaT keratinocytes in a CNR1 receptor-dependent manner (s7). Further, one of the key eCBs (i.e. anandamide; AEA) exhibited anti-allergic/anti-inflammatory effects in human skin, which could be abolished by CNR1 receptor inverse agonists falcarinol and rimonabant. These data, together with recent findings that activation of CNR1 in epidermal keratinocytes attenuated FITC-induced “atopic-like” dermatitis in a mouse model (s8), and that it limited the secretion of pro-inflammatory chemokines regulating T cell-dependent inflammation in the effector phase of contact hypersensitivity (s9),

strongly argue for that the ECS, and particularly the cutaneous eCB tone, plays a “gate-keeper” role in the initiation phase of skin inflammation.

Supplementary experimental design

Materials

AM251 and AM630 were purchased from Cayman Chemical Company (Ann Arbor, MI, USA); URB597, γ-irradiated lipopolysaccharides from *Escherichia coli* 026:B6 (LPS) and lipoteichoic acid from *Staphylococcus aureus* (LTA) were obtained from Sigma-Aldrich (St. Louis, MO, USA). Tacrolimus (Protopic®) was purchased from Astellas Pharma US, Inc. (Northbrook, IL, USA), whereas WOBE440 and WOBE479 were provided by Dr. August Wolff GmbH & Co. KG Arzneimittel (Bielefeld, Germany). AM251 was dissolved in absolute ethanol (Sigma-Aldrich), while the solvent for AM630, URB597, WOBE440 and WOBE479 was dimethyl sulphoxide (DMSO; Sigma-Aldrich). LPS and LTA were dissolved in filtered distilled water. In the case of the animal experiments, WOBE440 and WOBE479 were dissolved in the 4:1 mixture of acetone and olive oil. Tacrolimus was applied in a formulation of mineral oil, paraffin, propylene carbonate, white petrolatum and white wax.

Where applicable, in case of our *in vitro* experiments, AM251 and AM630 were applied 20 minutes in advance, whereas the FAAH-inhibitors (URB597, WOBE440 and WOBE479) and the LTA were administered simultaneously.

Cell culturing

Human immortalized keratinocytes (HPV-KER; 7,8), as well as primary normal human epidermal keratinocytes (NHEKs) were cultured in serum-free EpiLife medium (Life Technologies Hungary Ltd., Budapest, Hungary) supplemented with Human Keratinocyte Growth Supplement (HKGS; in 1:100; Life Technologies Hungary Ltd.),

antibiotics (preformed mixture of penicillin and streptomycin in 1:100; PAA Laboratories GmbH., Pasching, Austria) and Fungizone® Antimicotic (in 1:200; Life Technologies Hungary Ltd.).

Human skin samples were obtained after obtaining written informed consent from healthy individuals undergoing dermatosurgery, adhering to Helsinki guidelines, and after obtaining Institutional Research Ethics Committee's and Government Office for Hajdú-Bihar County's permission (protocol No.: DE OEC RKEB/IKEB 3724-2012; document No.: IX-R-052/01396-2/2012). NHEKs were isolated after overnight dermo–epidermal separation in 2.4 IU/ml dispase (Roche Diagnostics, Berlin, Germany) by short trypsin (0.05%, Sigma-Aldrich) digestion. Cells were cultivated at 37°C in humidified, 5% CO_2 containing atmosphere, the medium was changed every other day, and cells were sub-cultured at 70-80% confluence in both cases.

Determination of cellular viability

The viability of the cells was determined by measuring the conversion of the tetrazolium salt MTT (Sigma-Aldrich) to formazan by mitochondrial dehydrogenases. Cells were plated in 96-well plates (20,000 cells/well) in quadruplicates, and were cultured for 8, 24 or 72 hours. Cells were then incubated with 0.5 mg/ml MTT for 2 hrs, and concentration of formazan crystals (as an indicator of number of viable cells) was determined colorimetrically as described previously (s10-11). Results were expressed as percentage of vehicle controls regarded as 100%. When applicable, curve fitting was performed by Origin Pro Plus 6.0 software (Microcal, Northampton, MA, USA) using "Exponential Decay 1" curve fitting option.

RNA isolation, reverse transcription, quantitative "real-time" PCR (Q-PCR)

Q-PCR was performed as described previously (s11). Briefly, measurements were run on an ABI Prism 7000 sequence detection system (Applied Biosystems, Foster City, CA, USA) or Stratagene Mx3005P QPCR System (Agilent Technologies, Santa Clara, CA, USA) using the 5' nuclease assay. Total RNA was isolated using TRIzol (Life Technologies Hungary Ltd., Budapest, Hungary), DNase treatment was performed according to the manufacturer's protocol, and then 1 µg of total RNA were reverse-transcribed into cDNA by using High Capacity cDNA Kit from Life Technologies Hungary Ltd.. PCR amplification was performed by using TaqMan primers and probes (assay ID-s: Hs00155015_m1 for *FAAH*, Hs00174092_m1 for *IL1A*, Hs00174097_m1 for *IL1B*, Hs00985639_m1 for *IL6* and Hs00174103_m1 for *IL8*) and the TaqMan universal PCR master mix protocol (Applied Biosystems). As internal controls, transcripts of *peptidylprolyl isomerase A* (*cyclophilin A*; *PPIA*) were determined (assay ID: Hs 99999904_m1). The amount of the transcripts was normalized to those of the housekeeping gene using the ΔCT method. When indicated, the results were then normalized to the expression of the vehicle control (ΔΔCT method).

Western blotting

Cells were harvested in lysis buffer (20 mM Tris-HCl, pH 7.4, 5 mM EGTA, 1 mM 4-(2-aminoethyl) benzensulfonyl fluoride, protease inhibitor cocktail diluted 1:100, (all from Sigma-Aldrich) and the protein content was measured by a modified BCA protein assay (Pierce, Rockford, IL, USA). The samples were then subjected to sodium dodecyl sulfate-polyacrylamide gel electrophoresis. 10% Mini Protean TGX gels (Bio-Rad,

Hercules, CA, USA) were loaded with equal (28 µg) amount of protein per lane. Samples were then transferred to nitrocellulose membranes, by using Trans-Blot® Turbo™ Nitrocellulose Transfer Packs and Trans-Blot Turbo™ System (both from Bio-Rad), and then probed with rabbit-anti-human FAAH specific primary antibodies (Novus Biologicals, LLC, Littleton, Co, USA; in 1:250 dilution in 5% milk containing PBS). As secondary antibody, horseradish peroxidase-conjugated rabbit IgG Fc segment-specific antibodies (developed in goat, 1:1000 in 5% milk containing PBS, Bio-Rad) were used, and the immunoreactive bands were visualized by a SuperSignal® West Pico Chemiluminescent Substrate enhanced chemiluminescence kit (Pierce) using a KODAK Gel Logic 1500 Imaging System (Eastman Kodak Company, Kodak, Tokyo, Japan). To assess equal loading, membranes were re-probed with rabbit-anti-β-tubulin (TUBB) antibodies (1:1000, Novus Biologicals, LLC) and visualized as described above. Semiquantitative densitometric analysis of the signals was performed by using KODAK Molecular Imaging Software (Eastman Kodak Company, Rochester, NY, USA) or by using Image J software (National Institutes of Health, Bethesda, MD, USA).

Determination of the FAAH-activity

[ethanolamine-1-^{3}H]-AEA (60 Ci/mmol) was purchased from American Radiolabeled Chemicals Inc. (St. Louis, MO, USA). Anandamide and (3-aminocarbonyl)[1,1-biphenyl]-3-yl)-cyclohexylcarbamate (URB597) were purchased from Cayman Chemicals Europe. Tris·HCl and EDTA were ordered from Sigma-Aldrich (Switzerland). Ultima Gold liquid scintillation cocktail was purchased from Perkin Elmer (Switzerland).

The enzymatic activity of FAAH in NHEK and HPV-KER cell homogenates was assessed by determination of the hydrolysis of [ethanolamine-1-^{3}H]AEA as previously

described (s12-16). NHEK and HPV-KER homogenates (100 µg per sample) were incubated for 15 min at 37°C in 10 mM Tris·HCl, 1 mM EDTA (pH 9) with 5 µl vehicle (DMSO) or URB597 (final concentration: 100 nM) in a total volume of 500 µl. AEA was added as substrate using 5 µl of a mixture of [^{3}H]AEA (0.5 nM) plus unlabeled AEA (final concentration: 10 µM). The reaction was stopped after 10 min by addition of 1 ml ice-cold $CHCl_3$:MeOH (1:1) and vigorous vortexing. The aqueous phase was collected after phase separation by centrifugation at 10,000 g at 4°C for 10 min. The radioactivity of produced [^{3}H-ethanolamine] was measured by liquid scintillation counting on a Tri-Carb 2100 TR liquid scintillation analyzer after addition of 3.5 ml Ultima Gold scintillation cocktail (PerkinElmer Life Sciences). The background was determined using buffer alone without homogenate and subtracted from all samples. Data are reported as mean values of n ≥ 3 independent experiments each of them performed in triplicates.

Determination of apoptosis

A decrease in the mitochondrial membrane potential is one of the earliest markers of apoptosis. Therefore, to assess the process, mitochondrial membrane potential of HPV-KERs was determined using a MitoProbe™ $DiIC_1(5)$ Assay Kit (Life Technologies Hungary Ltd.). Cells (20,000 cells/well) were cultured in 96-well black-well/clear-bottom plates (Greiner Bio One, Frickenhausen, Germany) in quadruplicates and were treated with various compounds for 8-24 hrs. After removal of supernatants, cells were incubated for 30 minutes with $DiIC_1(5)$ working solution (50 µl/well), then washed with PBS, and the fluorescence of $DiIC_1(5)$ was measured at 630 nm excitation and 670 nm emission wavelengths using the FlexStation^{384} II or FlexStation 3 **FL**uorescence **I**mage Micro**P**late **R**eaders (FLIPRs; Molecular Devices, San Francisco, CA). Relative

fluorescence values were expressed as percentage of vehicle controls regarded as 100%.

Determination of necrosis

Necrotic processes were determined by SYTOX Green staining (Life Technologies Hungary Ltd.). The dye is able to penetrate (and then bind to the nucleic acids) only to necrotic cells with ruptured plasma membranes, whereas healthy cells with intact surface membranes show negligible SYTOX Green staining. Cells were cultured in 96-well black-well/clear-bottom plates (Greiner Bio One), and treated with various compounds for 8-24 hrs. Supernatants were then discarded, and the cells were incubated for 30 minutes with 1 µM SYTOX Green dye. Following incubation, cells were washed with PBS, the culture medium was replaced, and fluorescence of SYTOX Green was measured at 490 nm excitation and 520 nm emission wavelengths using FLIPR (Molecular Devices). $DiIC_1(5)$ and SYTOX Green labeling were performed as co-labeling of the same samples.

Experiments on NC/Tnd mice

The study was conducted at BioTox Sciences (BTS; San Diego, CA, USA). The study design and animal usage were reviewed and approved by the Institutional Animal Care and Use Committee (IACUC; No. 1109-05) for compliance with regulations prior to study initiation. Animal welfare was in compliance with the Guide for the Care and Use of Laboratory Animals and BioTox Sciences SOPs. All experiments on the animals were designed and performed by adopting the principles of “Guide for the Care and Use of Laboratory Animals, 8th Edition. National Academy Press, Washington, DC, 2010”.

8–9 weeks old male NC/Tnd mice (previously often referred to as NC/Nga; 9) were involved into the study. Mice were exposed to dust mite antigen as necessary to initiate the development of the disease condition. A standardized mixture of dust mite extracts (15,000 AU/ml of *Dermatophagoides pteronyssinus* and *D. farinae*) was used (Hollister-Stier Laboratories, Spokane, WA, USA). Animals were randomized on the basis of the average total clinical disease score for each group (approximately 1), and then treated for 30 days with vehicle (4:1 mixture of acetone:olive oil) or test substances. Clinical score was determined from observations of the upper back/lower neck (i.e., the area that received topical treatment) with a scale of 0–3 (0: absent; 1: mild; 2: moderate; 3: severe) for erythema, edema or papulations, and for oozing, crusts or hemorrhages. Each mouse received a single daily topical dose that was applied to the upper back/lower neck area. The study was run in two equal halves, each starting with N=4–5 animals. Evaluation of total disease score and measurement of ear thickness was performed as indicated (twice a week).

Determination of cytokine release (ELISA)

Cells were treated as indicated for 24 hours. Supernatants were collected, and the released amount of IL6, and IL8 was determined using OptEIA kits (BD Pharmingen, Franklin Lakes, NJ, USA) according to the manufacturer's protocol.

Statistical analysis

Data were analyzed and graphs were plotted by using Origin Pro Plus 6.0 software (Microcal, Northampton, MA, USA), using Student's two-tailed two samples *t*-test and $P<0.05$ values were regarded as significant differences.

Supplementary Conclusion section 1

The human skin establishes a complex homeostatic barrier (i.e. physico-chemical, immunological, microbiological) which protects the body against physical, chemical or microbiological challenges (s22-24). The physico-chemical barrier functions are dependent on the precisely orchestrated co-ordination of various cutaneous functions, such as e.g. proliferation and differentiation of the epidermal keratinocytes, sebum production, etc. (s22-24). In addition, the organization of the immunological barrier is based on complex, multi-directional interactions between the cutaneous commensal microbiome and various skin cells (s1-6, s25-27). Indeed, dysregulation of the immunological barrier, leading to several inflammation-accompanied cutaneous diseases such as e.g. atopic dermatitis (AD), show extremely high (and ever increasing) prevalence in the industrial countries (s26).

For chronic cutaneous inflammatory diseases, there is still a need for the development of novel, efficient and safe topical drugs with an improved benefit-risk profile as compared to topical corticosteroids or calcineurin inhibitors. It is widely accepted that in cutaneous inflammatory diseases (e.g. in AD), dysregulation of the local, cutaneous immune system impairs the physico-chemical skin barrier, thereby greatly contributing to the progression of the disease and the worsening of the symptoms (s27-28).

Although epidermal expression of FAAH was described long ago (s29), our data are the first ones arguing for that this enzyme, via decreasing the anti-inflammatory eCB tone (and on the other hand, subsequently increasing concentration of the pro-inflammatory "AEA degradation product" AA) shifts the AEA/AA steady-state towards a pro-inflammatory direction (**Supplementary Figure 7a-b**).

We found that activity (but not mRNA expression) of FAAH was strongly up-regulated upon TLR2-activation indicating that TLR2-coupled signaling plays a key role in the post-transcriptional regulation of FAAH (**Supplementary Figure S2**; **Figure 1a-f**). Furthermore, we also showed that inhibition of FAAH led to significant anti-inflammatory actions (**Figure 2a-d**) via the indirect (5,6) activation of CNR1 and CNR2 (**Supplementary Figure S3**). Moreover, we could also demonstrate that FAAH-inhibitors significantly ameliorated the cutaneous symptoms and reduced ear thickness of NC/Tnd mice, with an efficiency comparable to tacrolimus (**Figure 2e-f**; **Supplementary Figure S6a-d**), without any obvious macroscopic or behavioral side-effects in the course of the one month long treatment period. Thus, FAAH might provide an important (and previously un-described) contribution to the cutaneous inflammatory responses. These data invite further, extensive studies to unveil whether disturbed FAAH expression pattern and activity might indeed play a role in the pathogenesis of inflammation-accompanied skin diseases. Considering all these intriguing findings, inhibition (and thereby normalization) of TLR2-activation-induced epidermal FAAH-activity appears to be a highly targeted approach in restricting cutaneous inflammation.

Supplementary Conclusion section 2

Epidermal keratinocytes, via the controlled release of pro-inflammatory cytokines, are key players in the recruitment and activation of “professional” immune cells (s25); the regulation of their immunological activities is a crucial check-point of the initiation and orchestration of cutaneous inflammatory processes leading to the clinical signs of dermatitis. However, besides the expected keratinocyte-specific beneficial effects of the topically applied FAAH-inhibitors, one should also take into consideration the putative

effects of the elevated eCB-tone on the “professional” cutaneous immune cells. Indeed, elevation of the epidermal eCB tone, besides acting directly on the epidermal keratinocytes, may exert further anti-inflammatory actions by affecting epidermal Langerhans cells and sensory neurons (3), thereby contributing to the anti-inflammatory actions demonstrated in the *in vitro* part of our current study. Last, but not least, it is also noteworthy that topical administration of such inhibitors could also minimize the risk of systemic side-effects, holding out the promise of the development of novel, highly targeted, efficient, yet safe therapeutic tools.

Supplementary Figures

(**a**)

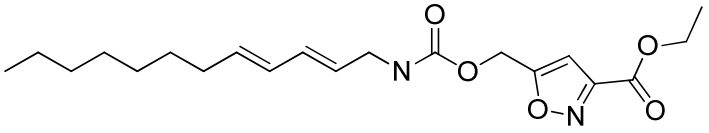

WOBE440

(**b**)

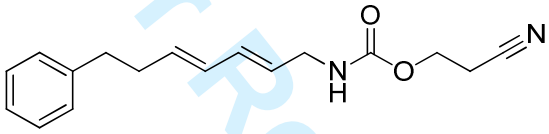

WOBE479

Supplementary Figure S1 *Chemical structures of the novel FAAH-inhibitors WOBE440 and WOBE479 (6)*

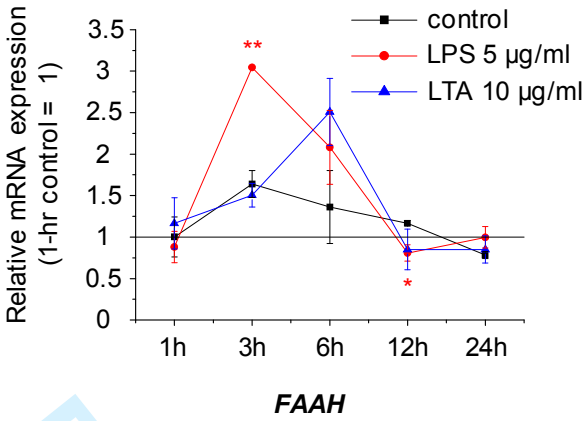

Supplementary Figure S2 *FAAH is expressed in HPV-KERs at the mRNA level*

FAAH mRNA expression of HPV-KERs following LPS, LTA (5 and 10 μg/ml, respectively) or vehicle treatments (1, 3, 6, 12 and 24 hrs). Data are presented by using the ΔΔCT method regarding *peptidylprolyl isomerase A* (*PPIA*)-normalized mRNA expression of the 1-hr control as 1 (solid line). Data are expressed as mean±SD of three independent determinations. One additional experiment yielded similar results.

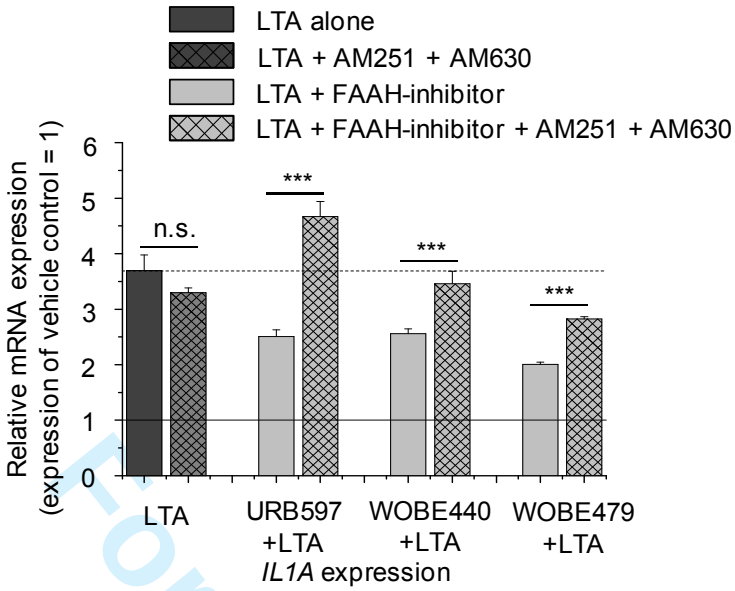

Supplementary Figure S3 *FAAH-inhibitors exert remarkable anti-inflammatory actions via activating CNR1 and CNR2 receptors*

Q-PCR analyses of HPV-KERs following the indicated 24-hr treatments (AM251: 1 μM; AM630: 1 μM; LTA: 10 μg/ml; WOBE440: 100 nM; WOBE479: 200 nM). Data are presented by using ΔΔCT method regarding *PPIA*-normalized mRNA expressions of the vehicle control as 1 (solid line). Data are expressed as mean±SD of 3 independent determinations. One additional experiment yielded similar results. ***P<0.001; n.s.: non-significant difference.

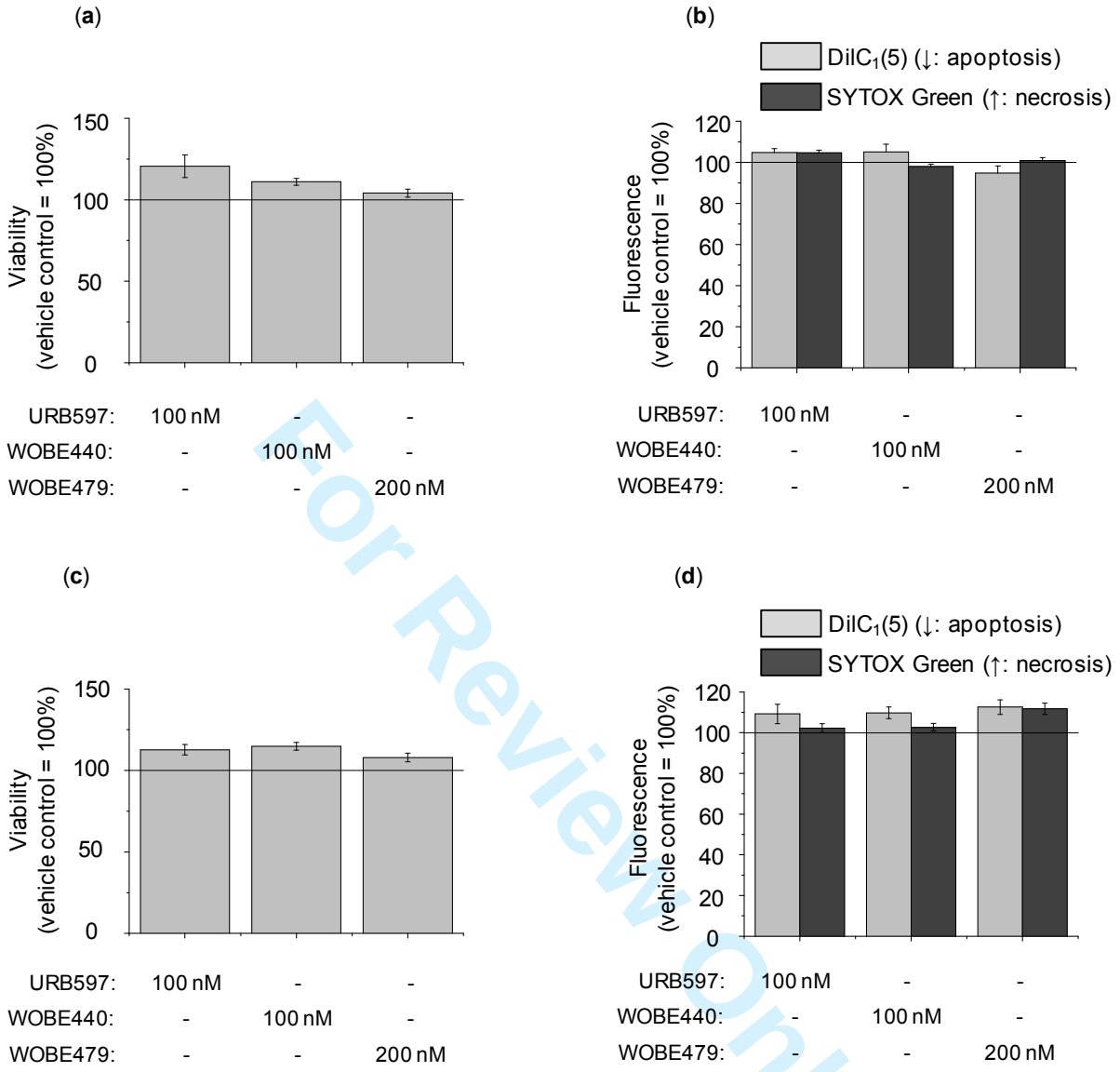

Supplementary Figure S4 *Effective anti-inflammatory concentrations of the FAAH-inhibitors are not cytotoxic*

(**a, c**) MTT-assays. Viability of HPV-KERs following 8- (**a**) or 24-hr (**c**) treatments. (**b**, **d**) Cell death ($DiIC_1(5)$-SYTOX Green double labeling of HPV-KERs) assays following 8- (**b**) or 24-hr (**d**) treatments. (**a**-**d**) Results are expressed in the percentage of the vehicle control (100%, solid line) as mean±SEM of four independent determinations. One additional experiment yielded similar results.

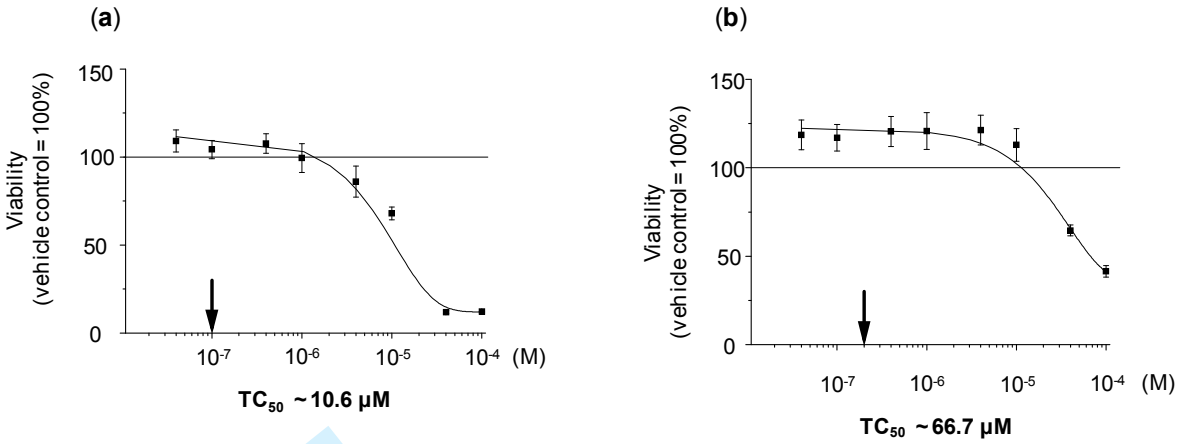

Supplementary Figure S5 *Effective anti-inflammatory concentrations of the novel FAAH-inhibitors are not cytotoxic even in case of long-term application*

(**a-b**) MTT-assays. Viability of HPV-KERs following 72-hr treatments. Results are expressed in the percentage of the vehicle control (100%, solid line) as mean±SEM of four independent determinations. One additional experiment yielded similar results. Arrows indicate the effective anti-inflammatory concentrations of the compounds. TC_{50}: the estimated half-cytotoxic concentration of the substances.

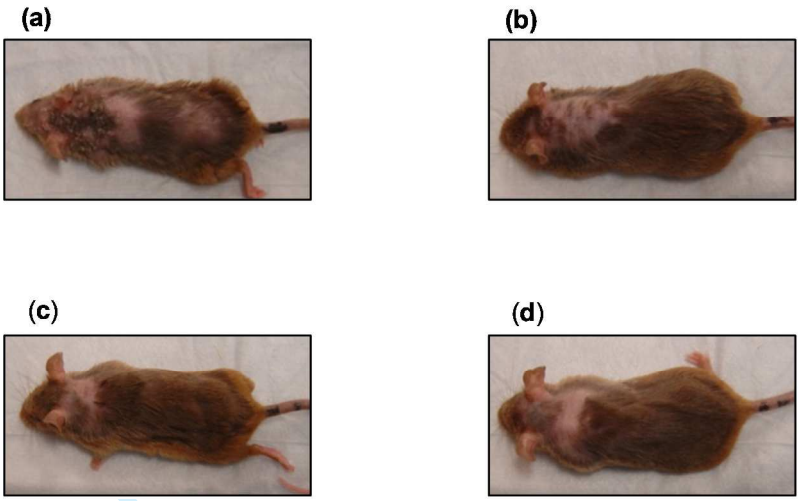

Supplementary Figure S6 *Topically applied FAAH-inhibitors improve symptoms of* NC/Tnd mice

Representative images of the animals at the end of the study period (1 month). (**a**) control group. (**b**) tacrolimus group. (**c**) WOBE440 group. (**d**) WOBE479 group.

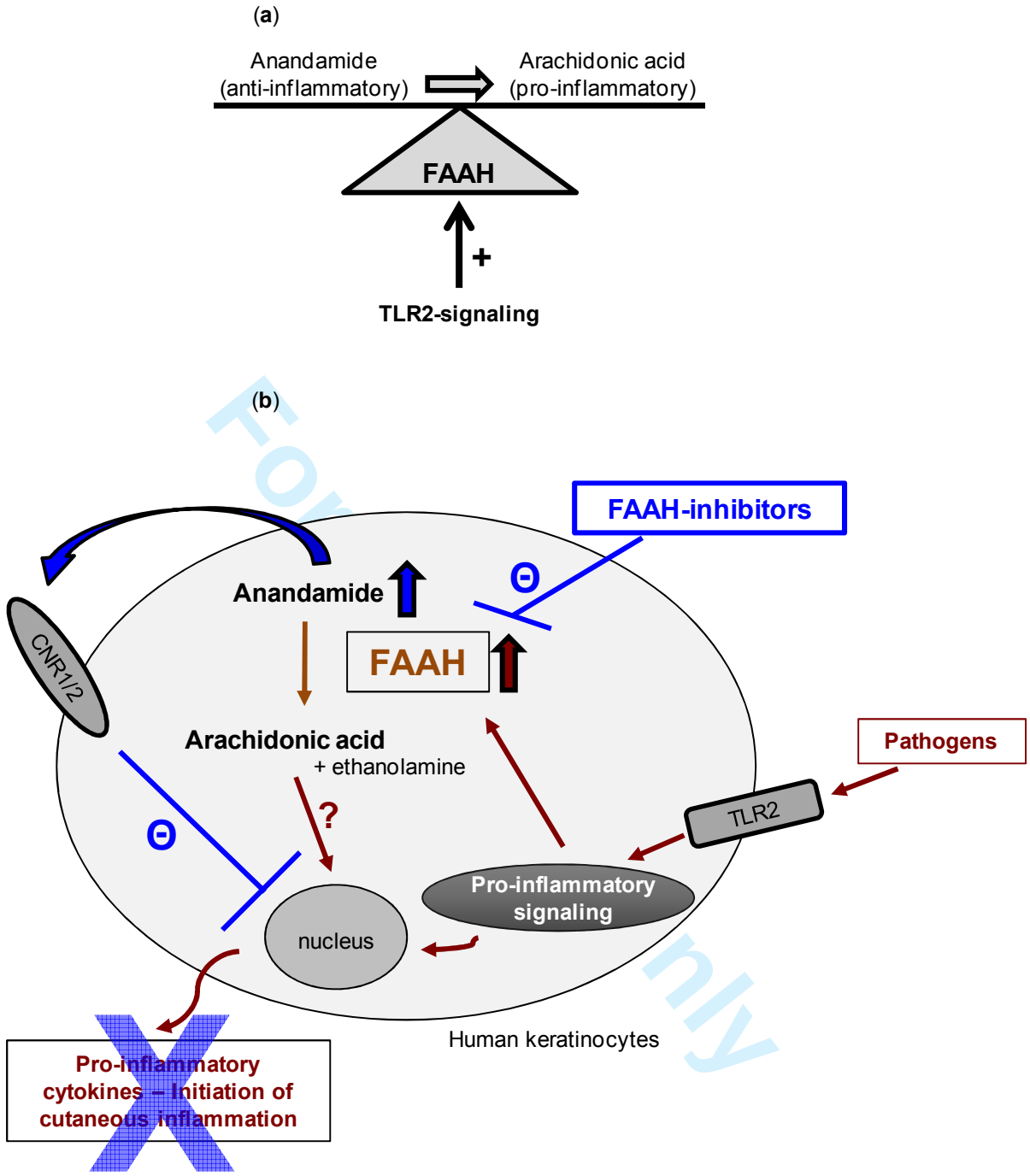

Supplementary Figure S7 *Overview of the role of FAAH in mediating cutaneous inflammation*

The inflammation-controlling "eCB steady-state" (**a**) and mechanism of the anti-inflammatory action of FAAH-inhibitors (**b**). Color codes: TLR2-activation mediated actions; effects of FAAH-inhibition; result of FAAH-activity.

Supplementary References

s1 Gallo R L, Nakatsuji T. Microbial symbiosis with the innate immune defense system of the skin. J Invest Dermatol 2011: **131**: 1974–1980.

s2 Wiesner J, Vilcinskas A. Antimicrobial peptides: the ancient arm of the human immune system. Virulence 2010: **1**: 440–464.

s3 Miller L S, Modlin R L. Human keratinocyte Toll-like receptors promote distinct immune responses. J Invest Dermatol 2007: **127**: 262–263.

s4 Lebre M C, Aar A M G van der, Baarsen L van *et al.* Human keratinocytes express functional Toll-like receptor 3, 4, 5, and 9. J Invest Dermatol 2007: **127**: 331–341.

s5 Meglio P Di, Perera G K, Nestle F O. The multitasking organ: recent insights into skin immune function. Immunity 2011: **35**: 857–869.

s6 Nestle F O, Meglio P Di, Qin J-Z *et al.* Skin immune sentinels in health and disease. Nat Rev Immunol 2009: **9**: 679–691.

s7 Leonti M, Casu L, Raduner S *et al.* Falcarinol is a covalent cannabinoid CNR1 receptor antagonist and induces pro-allergic effects in skin. Biochem Pharmacol 2010: **79**: 1815–1826.

s8 Gaffal E, Glodde N, Jakobs M *et al.* Cannabinoid 1 receptors in keratinocytes attenuate fluorescein isothiocyanate-induced mouse atopic-like dermatitis. Exp Dermatol 2014: **23**: 401–406.

s9 Gaffal E, Cron M, Glodde N *et al.* Cannabinoid 1 receptors in keratinocytes modulate proinflammatory chemokine secretion and attenuate contact allergic inflammation. J Immunol 2013: **190**: 4929–4936.

s10 Tóth B I, Dobrosi N, Dajnoki A *et al.* Endocannabinoids modulate human epidermal keratinocyte proliferation and survival via the sequential engagement of cannabinoid receptor-1 and transient receptor potential vanilloid-1. J Invest Dermatol 2011: **131**: 1095–1104.

s11 Oláh A, Tóth B I, Borbíró I *et al.* Cannabidiol exerts sebostatic and antiinflammatory effects on human sebocytes. J Clin Invest 2014: **124**: 3713–3724.

s12 Maccarrone M, Stelt M van der, Rossi A *et al.* Anandamide hydrolysis by human cells in culture and brain. J Biol Chem 1998: **273**: 32332–32339.

s13 Maccarrone M, Bari M, Agrò A F. A sensitive and specific radiochromatographic assay of fatty acid amide hydrolase activity. Anal Biochem 1999: **267**: 314–318.

s14 Maccarrone M, Valensise H, Bari M *et al.* Progesterone up-regulates anandamide hydrolase in human lymphocytes: role of cytokines and implications for fertility. J Immunol 2001: **166**: 7183–7189.

s15 Oddi S, Bari M, Battista N *et al.* Confocal microscopy and biochemical analysis reveal spatial and functional separation between anandamide uptake and hydrolysis in human keratinocytes. Cell Mol Life Sci 2005: **62**: 386–395.

s16 Nicolussi S, Viveros-Paredes J M, Gachet M S *et al.* Guineensine is a novel inhibitor of endocannabinoid uptake showing cannabimimetic behavioral effects in BALB/c mice. Pharmacol Res 2014: **80**: 52–65.

s17 Nasti T H, Timares L. Inflammasome activation of IL-1 family mediators in response to cutaneous photodamage. Photochem Photobiol 2012: **88**: 1111–1125.

s18 Stamatas G N, Morello A P, Mays D A. Early inflammatory processes in the skin. Curr Mol Med 2013: **13**: 1250–1269.

s19 Meisgen F, Xu Landén N, Wang A *et al.* MiR-146a negatively regulates TLR2-induced inflammatory responses in keratinocytes. J Invest Dermatol 2014: **134**: 1931–1940.

s20 Mor M, Rivara S, Lodola A *et al.* Cyclohexylcarbamic acid 3'- or 4'-substituted biphenyl-3-yl esters as fatty acid amide hydrolase inhibitors: synthesis, quantitative structure-activity relationships, and molecular modeling studies. J Med Chem 2004: **47**: 4998–5008.

s21 Reitamo S, Remitz A. An update on current pharmacotherapy options in atopic dermatitis. Expert Opin Pharmacother 2014: **15**: 1517–1524.

s22 Elias P M. Skin Barrier Function. Curr Allergy Asthma Rep 2008: **8**: 299–305.

s23 Rawlings A V. Recent advances in skin "barrier" research. J Pharm Pharmacol 2010: **62**: 671–677.

s24 Oláh A, Szöllősi A G, Bíró T. The channel physiology of the skin. Rev Physiol Biochem Pharmacol 2012: **163**: 65–131.

s25 Kupper T S, Fuhlbrigge R C. Immune surveillance in the skin: mechanisms and clinical consequences. Nat Rev Immunol 2004: **4**: 211–222.

s26 Kubo A, Nagao K, Amagai M. Epidermal barrier dysfunction and cutaneous sensitization in atopic diseases. J Clin Invest 2012: **122**: 440–447.

s27 Kuo I-H, Yoshida T, Benedetto A De *et al.* The cutaneous innate immune response in patients with atopic dermatitis. J Allergy Clin Immunol 2013: **131:** 266–278.

s28 Howell M D, Kim B E, Gao P *et al.* Cytokine modulation of atopic dermatitis filaggrin skin expression. J Allergy Clin Immunol 2009: **124**: R7–R12.

s29 Maccarrone M, Rienzo M Di, Battista N *et al.* The endocannabinoid system in human keratinocytes. Evidence that anandamide inhibits epidermal differentiation through CNR1 receptor-dependent inhibition of protein kinase C, activation protein-1, and transglutaminase. J Biol Chem 2003: **278**: 33896–33903.